

UCRL-JC--105626  
PREPRINT

Response Matrix Monte Carlo Based on a  
General Geometry Local Calculation  
for Electron Transport

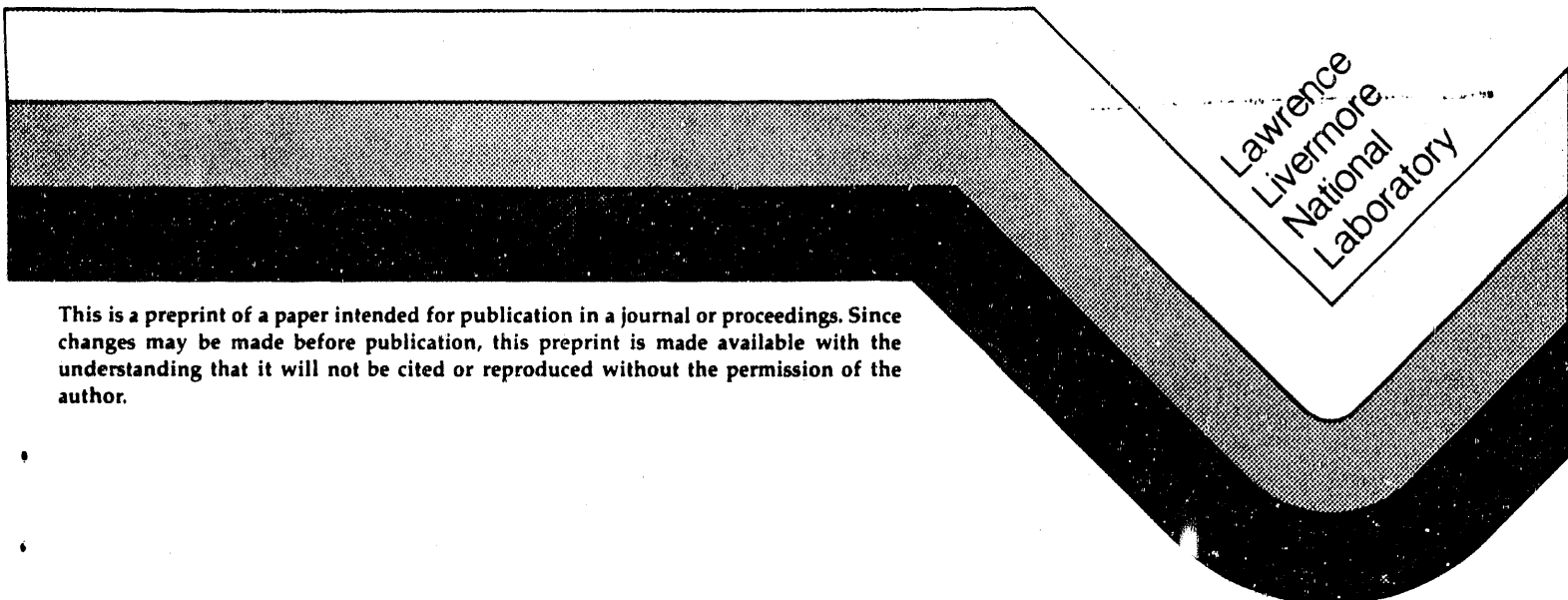
Clinton T. Ballinger  
James A. Rathkopf  
The Lawrence Livermore National Laboratory  
William R. Martin  
The University of Michigan

This paper was prepared for submittal  
to the Advances in Mathematics,  
Computations, and Reactor Physics  
Conference  
Pittsburgh, PA

Received by OSTI

FEB 19 1991

April 28-May 1, 1991



This is a preprint of a paper intended for publication in a journal or proceedings. Since changes may be made before publication, this preprint is made available with the understanding that it will not be cited or reproduced without the permission of the author.

#### **DISCLAIMER**

**This document was prepared as an account of work sponsored by an agency of the United States Government. Neither the United States Government nor the University of California nor any of their employees, makes any warranty, express or implied, or assumes any legal liability or responsibility for the accuracy, completeness, or usefulness of any information, apparatus, product, or process disclosed, or represents that its use would not infringe privately owned rights. Reference herein to any specific commercial products, process, or service by trade name, trademark, manufacturer, or otherwise, does not necessarily constitute or imply its endorsement, recommendation, or favoring by the United States Government or the University of California. The views and opinions of authors expressed herein do not necessarily state or reflect those of the United States Government or the University of California, and shall not be used for advertising or product endorsement purposes.**

## RESPONSE MATRIX MONTE CARLO BASED ON A GENERAL GEOMETRY LOCAL CALCULATION FOR ELECTRON TRANSPORT

Clinton T. Ballinger and James A. Rathkopf  
Lawrence Livermore National Laboratory  
P.O. Box 808, L-95  
Livermore, CA 94550

and

William R. Martin  
University of Michigan  
Nuclear Engineering Department  
Ann Arbor, MI 48109

### ABSTRACT

A Response Matrix Monte Carlo (RMMC) method has been developed for solving electron transport problems. This method was born of the need to have a reliable, computationally efficient transport method for low energy electrons (below a few hundred keV) in all materials. Today, condensed history methods are used which reduce the computation time by modeling the combined effect of many collisions but fail at low energy because of the assumptions required to characterize the electron scattering. Analog Monte Carlo simulations are prohibitively expensive since electrons undergo coulombic scattering with little state change after a collision. The RMMC method attempts to combine the accuracy of an analog Monte Carlo simulation with the speed of the condensed history methods. Like condensed history, the RMMC method uses probability distributions functions (PDFs) to describe the energy and direction of the electron after several collisions. However, unlike the condensed history method the PDFs are based on an analog Monte Carlo simulation over a small region. Condensed history theories require assumptions about the electron scattering to derive the PDFs for direction and energy. Thus the RMMC method samples from PDFs which more accurately represent the electron random walk. Results show good agreement between the RMMC method and analog Monte Carlo.

### INTRODUCTION

A Response Matrix Monte Carlo (RMMC) method has been developed for electron transport calculations in finite media. This new method is based on using energy, angle, and position probability distribution functions (PDFs) which are constructed from an analog Monte Carlo simulation over a small region (local calculation). Local calculations for different incident energies and region sizes generate PDFs for use in a global Monte Carlo calculation. In the global calculation, random samples from the PDFs are used to simulate the transport of electrons by updating electron energy, angle, and position. Unlike deterministic response matrix techniques, this method does not depend on *a priori* knowledge of global geometry. The geometry of the local calculation is independent of the overall geometry being analyzed. Hence, local calculations need to be performed only once so a data base can be constructed for different materials.

Electron transport problems are complicated by the extremely anisotropic coulombic scattering cross section and the very small energy loss associated with individual electron interactions. Condensed history methods, presently used for electron transport problems, combine the effects of many collisions into a composite effect that is more easily modeled in a Monte Carlo code. Generalizations about the scattering kernel and energy loss per collision are required to predict the composite effect. Low energy electron transport (below a few hundred keV) is ill-suited for condensed history because the scattering angle and energy loss are greater than at high energies. The RMMC method can be used as a replacement for condensed history methods especially at low energies where condensed history results are considered unreliable.

## ELECTRON INTERACTIONS

Electron interactions fall under two categories: inelastic scatter where the electron changes energy and direction, and elastic scatter, where only the direction changes. Inelastic events include ionization and excitation which alter the target atom by knocking out or exciting a bound electron. The target atom can relax or decay to produce secondary radiation in the form of Auger electrons or x-rays. When electrons impinge upon a material, a multiplication in the electron population occurs complicating the transport.

Coulombic interactions with the charged atomic nucleus have negligible effect on electron energy since the nucleus is many times heavier than an electron but the interactions can change the electrons direction. As energy decreases, the elastic scattering cross section dominates. Figure 1 shows the average scattering cosine associated with a single elastic scattering event ( $\mu$  is the cosine of the scattering angle). Because elastic scatter is extremely anisotropic especially at high energies, Legendre moments would be ineffective in describing the angular dependence unless hundreds of moments were used. Table 1 shows the total interaction cross section<sup>(1-4)</sup> compared to total photon interaction cross sections<sup>5</sup> as a function of energy. The electron cross sections are up to five orders of magnitude larger than the photon cross sections while the average energy loss per collision are sometimes five orders of magnitude lower. Total electron cross section refers to the sum of ionization, bremsstrahlung, and elastic scattering cross sections. Excitation cross sections, if included, would increase the difference between photons and electrons even more. Hence, electron transport does not lend itself to photon transport techniques.

## ANALOG MONTE CARLO

Analog Monte Carlo simulations for electron transport are prohibitively time consuming for all but the thinnest geometries since an electron undergoes thousands of collisions while traveling a fraction of its range. An analog Monte Carlo code has been written to generate input for the RMMC method and to test the accuracy of some condensed history models. Cross sections for ionization, elastic scatter and bremsstrahlung events were compiled into a data base and used in the analog simulation. Excitation events were modeled with a stopping power since excitation cross sections were unavailable at the time of this work. All cross sections are organized in a continuous energy format (ENDL format type) for all electron interactions and distributions describing elastic scatter deflection, knock-on electron energy, and bremsstrahlung photon energy are tabulated for distinct incident energies.

Equal probability bin structure describing the distributions would require large amounts of storage due to the extremely small energy and angle changes. Alternatively, the table look-up method would require less storage but sampling is very slow. Sampling speed is important since the Monte Carlo code will sample for thousands of collisions. The Alias method<sup>6</sup> was chosen instead of conventional sampling schemes for the analog Monte Carlo code since it is as accurate as table

look-up yet nearly as fast as equal probable bin sampling. Statistical interpolation is used to find outgoing electron characteristics for incident electrons with energies different from energies in which distributions are tabulated. Equation 1 summarizes the statistical interpolation technique when E is the electron energy and the distribution varies linearly in energy.

$$R = \frac{E_i - E}{E_i - E_{i-1}} \quad (E_{i-1} < E < E_i) \quad (1)$$

if  $R \geq \xi$  then sample from the  $E_i$  distribution

if  $R < \xi$  then sample from the  $E_{i-1}$  distribution

$\xi$  = random variable  $\in [0,1)$

### CONDENSED HISTORY MONTE CARLO

To avoid the computational requirements of an analog Monte Carlo simulation, condensed history methods were developed. Many condensed history theories exist which describe energy and direction distributions for electrons that have traveled a short path-length. For Example, theories by Moliere <sup>7</sup> and Goudsmit & Saunderson <sup>8</sup> are used to describe the electron direction while the theory by Landau <sup>9</sup> describe the exit energy distribution. The combination of these theories gives a complete description of the electron direction and energy after a certain path-length.

The idea behind condensed history methods is that PDFs representing energy and direction can be generated to describe the effect of many collisions over a short path-length. In a Monte Carlo code these PDFs can be sampled to reconstruct electron histories over a larger region. Thus, individual events are replaced by sampling from a PDF that represents the result of a large number of collisions in the Monte Carlo code. Assumptions that limit the electron scattering are required since the PDFs are obtained analytically. Moliere assumed small angle scatter for individual collisions to obtain an expression for the angle distribution after several collisions. The theory of Goudsmit & Saunderson uses the small angle approximation by claiming the number of collisions is given by a Poisson distribution as shown in Equation 2. This is only true when the physical dimension is equivalent to the path-length traveled by the electron.

$$P(n) = e^{-\Sigma_t d} (\Sigma_t d)^n / n! \quad (2)$$

Where:

$P(n)$  = probability of n collisions

d = distance traveled

$\Sigma_t$  = total macroscopic cross section

Figure 2 shows that this condition can be met only if each collision causes no angle change, ie. small angle approximation. The use of the small angle assumption implies that the theories are based on conditions which do not exist at low energy since the mean scattering angle increases exponentially with decreasing energy, Figure 1. In light of the assumptions used, the condensed history theories are outside their range of validity at low energies. The energy where the condensed history methods fail is dependent upon material thickness and atomic number.

### RESPONSE MATRIX MONTE CARLO

Like the condensed history theories, the RMMC method develops PDFs for direction and energy which represent the effect of many collisions. The RMMC method generates these distributions using an analog Monte Carlo simulation. Position distributions are also constructed since the

electrons are not assumed to go straight, giving the advantage of producing PDFs which are valid for any energy. The RMMC method consists of two codes, an analog Monte Carlo code to generate the PDFs (local calculation) and a RMMC code that uses these PDFs to step through a large problem (global calculation).

## LOCAL CALCULATION

PDFs are generated in the local calculation via an analog Monte Carlo simulation of electron transport over a small region. PDFs for energy, direction, and position are constructed and assumed independent of one another so that storage is reduced by avoiding coupled energy-direction-position distributions. Decoupling the variables introduces inaccuracies in the global calculation. Local region shape determines the extent of the coupling between energy and direction with position. Slab geometry local regions are not suited for construction of independent PDFs because the strong relation of energy on exit position. Electrons can suffer a variety of different histories in the slab geometry since those escaping straight do not encounter as many collisions as those exiting at a corner.

The ideal shape would be a surface of equal path-lengths, where all exiting electrons have traveled the same distance allowing energy and position to be nearly decoupled. Spherical geometry provides a good approximation to the equal path-length surface. Hemisphere local calculations were chosen for this work because the problems of interest are beams incident upon flat surfaces. In addition, few electrons scatter in the backward direction making it computationally inefficient to track a few renegade electrons in the reverse direction since little additional information is gained. The local calculations are considered to be independent of overall problem geometry since various sized hemispheres can be used to roughly fit any geometry. Traditional response matrix techniques call for a problem specific local calculation to fit the geometry whereas the use of hemispheres allows all geometries to be analyzed. Results from different sized hemispheres are easily obtained by tallying as the electrons cross different radial boundaries. Full radius hemispheres are on the order of 100 mean free path-lengths in radius; half radius hemispheres are constructed in the same calculation. The hemisphere surfaces were divided into sections where energy and angle PDFs were constructed by tallying the electrons that exit a particular section, Figure 3.

Tallying over a surface section preserves some of the coupling of position with energy and angle. Three dimensional quantities such as direction and position require a close investigation to reveal symmetry which can reduce the number of coupled tallies. The exit position PDF has an obvious symmetry because the cross sections are azimuthally symmetric; the exit position angle ( $\phi$ ) is enough to describe the exit position, Figure 4. A complete description of the particle direction requires a coupled recording of two direction cosines. Since this would require a large amount of storage, simplifications are made to reduce the distribution to one variable. Detailed tallying of the exit directions revealed the existence of a subtle symmetry. The exit direction is symmetric about the  $n$ - $\tau$  plain in Figure 4 where  $n$  is the surface normal and  $\tau$  is tangent to the hemisphere and intersects the incident axis.

A PDF representing the electron projected angle onto the  $n$ - $\tau$  plain was required to describe exiting direction. The direction in the  $n$ - $\gamma$  plain can be approximated by a Gaussian with a small width. These two direction cosines can be used to reconstruct the third direction cosine; hence, only one PDF is required to describe the 3-D direction.

## GLOBAL CALCULATION

Once the PDFs from several local calculations for different incident energies and sizes are constructed, the global calculation can proceed. Statistical interpolation is used for electron energies between energies where PDFs are tabulated. The global simulation begins by sampling an exit position cosine and placing it randomly in azimuth on the hemisphere. This position indicates

which of the divided surface sections should be used when sampling from the energy and exit direction PDFs. Once the energy and direction are updated by sampling from the correct PDFs for the surface section, the new electron state is fully described.

This process is continued until the electron encounters a boundary or the energy falls below a cutoff energy. Figure 5 shows what a single electron history might look like in the global calculation. Boundaries cannot be matched exactly with hemispheres but are approximated by using smaller hemispheres. When a boundary is crossed, the sampled exit position is used to indicate the direction of exit from the global calculation and the energy loss is taken as a fraction of the sampled energy loss. A linear relation between energy loss and distance to the boundary is assumed.

## RESULTS

### VALIDITY OF THE ANALOG MONTE CARLO CODE

The analog Monte Carlo code results were compared to MCNP4<sup>10</sup>, SANDYL<sup>11</sup>, and to various experimental results to establish its validity. This was required before performing local calculations for the RMMC method. It is useful to note that condensed history methods, including MCNP4 and SANDYL, are not expected to perform well for transporting electrons with energies in the keV range and for backscattering problems. Figure 6 shows the backscattered energy spectrum for 10 keV electrons normally incident on thick aluminum. Notice the analog Monte Carlo results compare well with experimental data from Darlington, *et al.*<sup>12</sup> while the results from MCNP4 do not fair as well. Table 2 shows the amount of saturation backscatter predicted by the analog Monte Carlo code compared to the Darlington data.

Notice that the experimental data falls within the statistics of the analog Monte Carlo results except for the 9.3 keV incident energy. However, this discrepancy does not invalidate the analog results since the experiment may count electrons that have energy less than 0.1 keV which is the low energy cutoff for the analog code. There are uncertainties with the measured results as well which could account for the slight difference in backscatter percentage. Other comparisons between experimental data and the analog code show similar good agreement for various energies and materials.

### VALIDITY OF THE RESPONSE MATRIX MONTE CARLO CODE

MCNP4, SANDYL, and the analog Monte Carlo code results along with experimental data were compared to the response matrix results. Figure 7 show the backscatter percentage verses incident energy for electrons normally incident on thick aluminum. The error bars indicated on the response matrix results were calculated based on the global statistics. No consideration was given for the statistical nature of the local calculation which generated the PDFs used in the global calculation. The SANDYL results<sup>13</sup> underestimate the experimental results especially at energies below 100 keV. The response matrix results lie within statistical error of the experimental results except for energies below 20 keV. The RMMC backscatter results are at least as good as the MCNP4 results which also deviate from the experimental data below 20 keV.

The transmitted energy spectrum for electrons exiting a slab of aluminum was also used to compare the RMMC results to the analog code and MCNP4. Figure 8 shows the good agreement between the methods in predicting the exiting energy spectrum. Other comparisons between the RMMC results and the analog code results show good agreement for exit location, direction and energy on the transmitted and backscatter planes. Table 3 shows some execution time comparisons between

the RMMC method, the analog simulation, and MCNP4. It is not surprising that the response matrix results are on the order of 70 times faster than the analog Monte Carlo results since the local calculations are roughly 70 mean free pathlengths thick for energies greater than 30 keV. The RMMC method can be speeded up simply by using larger radius hemispheres when performing the local calculations. Rates listed in Table 3 for the RMMC method do not consider computation time for the local calculations. The MCNP4 calculation rate is about the same as the response matrix method. Thus, the hemisphere sizes that were chosen must be about the same as the sub-step size in MCNP4.

## CONCLUSIONS

The analog Monte Carlo code reproduced experimentally measured data for different incident energies in aluminum. Exiting energy distributions, exit location, and direction predicted in the analog Monte Carlo code all compared very well to experimental data. This code was then used to generate accurate PDFs describing the energy, position, and direction of electrons escaping a local region. The RMMC method was successfully used to reproduce analog Monte Carlo results in a fraction of the time. The method performed at least as well as MCNP4 for predicting the energy spectrum for backscattered and transmitted electrons and out-performed SANDYL predicting low energy backscatter percentages. The RMMC method did not compare well with experimental data and analog Monte Carlo results for the backscatter percentage below 25 keV. An effort is underway to determine why there is a difference between the analog Monte Carlo and RMMC for these low energies. No step size adjustments were used in the condensed history codes for this comparison. Condensed history theories are not expected to perform well in high atomic number (Z) materials because the scattering angle becomes larger, making the assumptions used in the condensed history derivations invalid. The condensed history results and the response matrix results will show greater disagreement in high Z materials. Since the response matrix method is free from material property assumptions, it should reproduce the analog Monte Carlo results as closely for high Z material as it did for aluminum. The RMMC method is many times faster than analog Monte Carlo. The speedup depends on how many mean free pathlengths are represented in each local calculation. Hence, the larger the size of the local calculation, the faster the RMMC method can simulate the global transport.

## ACKNOWLEDGEMENTS

The author is grateful to Dermott E. Cullen and Sterrett T. Perkins for illuminating discussions concerning electron interactions and for providing the data base for the analog Monte Carlo code. This work was performed under the auspices of the U.S. Department of Energy by Lawrence Livermore National Laboratory under contract No. W-7405-Eng-48.



## REFERENCES

- 1) D.E.Cullen and S.T.Perkins, "The Livermore Bremsstrahlung Data Base," Lawrence Livermore National Laboratory, Livermore, CA, UCID-21627 (1989).
- 2) S.T.Perkins and D.E.Cullen, "The Livermore Electron Impact Ionization Data Base," Lawrence Livermore National Laboratory, Livermore, CA, UCID-21628 (1990).
- 3) S.T.Perkins and D.E.Cullen, "The Livermore Electron Elastic Scattering Data Base," Lawrence Livermore National Laboratory, Livermore, CA, UCRL-ID-103170 (1990).
- 4) S.T.Perkins, M.H.Chen, D.E.Cullen, and J.A.Rathkopf, and J.H.Scofield, "The Livermore Evaluated Atomic Data Library (EADL)," Lawrence Livermore National Laboratory, Livermore, CA, UCRL-50400 Vol. 30 (to be published 1990).
- 5) D.E.Cullen, M.H.Chen, J.H.Hubbell, S.T.Perkins, E.F.Plechaty, J.A.Rathkopf, and J.H.Scofield, "Tables and Graphs of Photon Interaction Cross Sections from 10 eV to 100 GeV Derived from the LLNL Evaluated Photon Data Library (EPDL)," Lawrence Livermore National Laboratory, Livermore, CA, UCRL-50400 Vol. 6 Rev. 4 (1990).
- 6) A.L.Edwards, J.A. Rathkopf, and R.K.Smidt, "Extending the Alias Monte Carlo Sampling Method to General Distributions," to appear in the proceedings from this conference.
- 7) M.J.Berger, "Monte Carlo Calculation of the Penetration and Diffusion of Fast Charged Particles", Methods in Computational Physics, Vol. 1, 135-215 (1963).
- 8) S. Goudsmit and J.L.Saunderson, "Multiple Scattering of Electrons", Phys. Rev. 57, pp. 24-29 (1940).
- 9) L.Landau, "On the energy loss of fast particles by ionization," J. Phys., USSR, 8 (No.4), pp. 201-205 (1944).
- 10) J.F.Briesmeister, Editor, "MCNP4 - A General Monte Carlo Code for Neutron, Photon, and Electron Transport", LANL, (1990).
- 11) H.M.Colbert, "SANDYL A Computer Program for Calculating Combined Photon - Electron Transport in Complex Systems", SLL-74-0012, SNL-Livermore, (1974).
- 12) E.H.Darlington, (1975), "Backscattering of 10-100 keV Electrons from Thick Targets", J. Phys. D Appl. Phys., Vol. 8, pp. 85-93.
- 13) A.J.Antolak and W.Williamson, Jr., "Electron Backscattering from Bulk Materials", Sandia Report SAND84-8969, (1985)

**Table 1. Cross Sections and Energy Losses for Electron and Photon Interactions**

Energy (MeV)	Electron total $\sigma$ (barns)	Electron Fractional $\Delta E/E$	Photon total $\sigma$ (barns)
10000	3.25E6	2.0E-5	1.4192
1000	3.31E6	2.0E-5	1.3579
100	3.42E6	2.0E-5	1.1268
10	4.19E6	2.6E-5	1.0365
1.0	9.05E6	3.9E-5	2.7510
0.1	3.90E7	1.8E-4	7.6413
0.01	1.07E8	1.5E-3	1167.2
0.001	6.03E8	0.011	5.2837E4
0.0001	1.09E9	0.052	5.7659E6

**Table 2. Backscatter Coefficients for Normally Incident Electrons on Thick Aluminum**

Energy (keV)	Darlington	Analog Monte Carlo
9.3	18.1	17.4 $\pm$ 0.42
11	17.9	18.0 $\pm$ 0.42
25.2	16.1	15.9 $\pm$ 0.40
62.1	15.0	14.9 $\pm$ 0.39
102	14.7	14.5 $\pm$ 0.38

**Table 3. Calculation Rate for Normally Incident Electrons on Thick Aluminum Given as Number of Histories/cpu second on a Cray YMP**

Energy (keV)	MCNP4 #/sec	RMMC #/sec	Analog MC #/sec
200	106.1	151.2	N/A
100	124.9	216.5	3.07
70	130.0	250.1	3.57
25.2	183.3	490.2	6.73
10	263.1	680.3	24.5

Figure 1. Mean Scattering Angle Verses Electron Kinetic Energy.

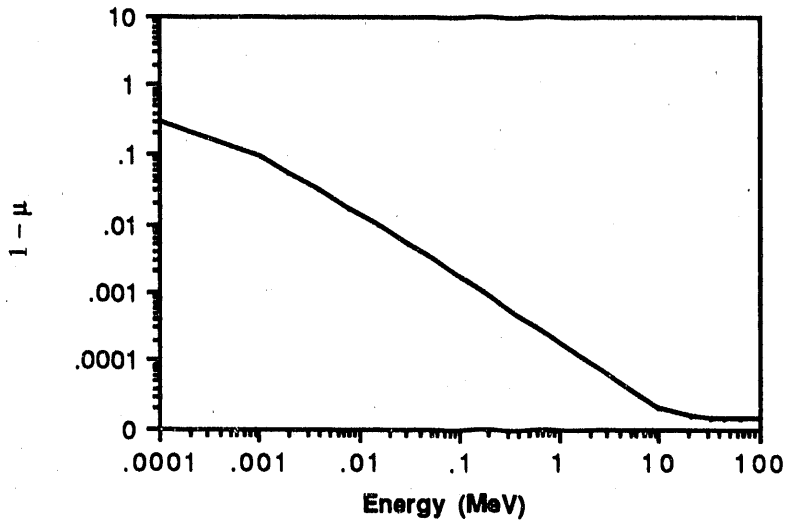


Figure 2. Path-Length not Equal to the Straight Ahead Distance.

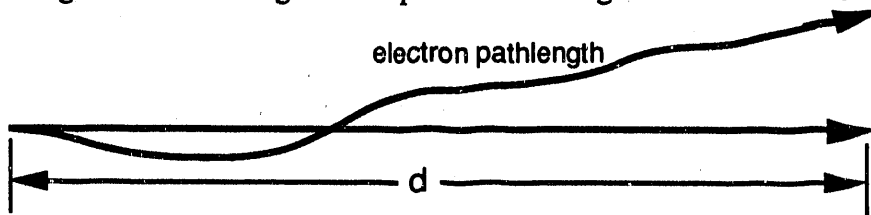


Figure 3. Sectioned Hemisphere Used for the Local Calculations.

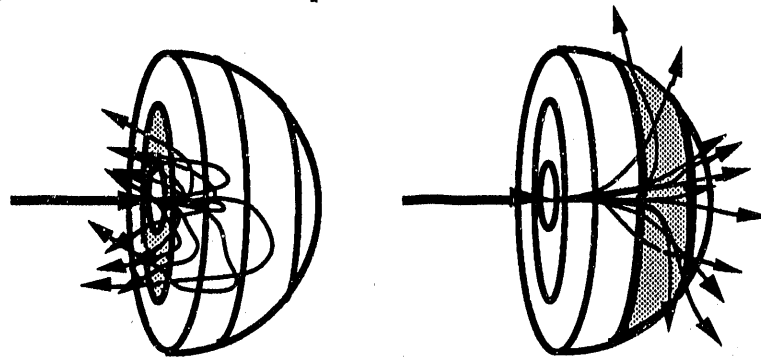


Figure 4. Exit Position and Exit Direction Symmetry.

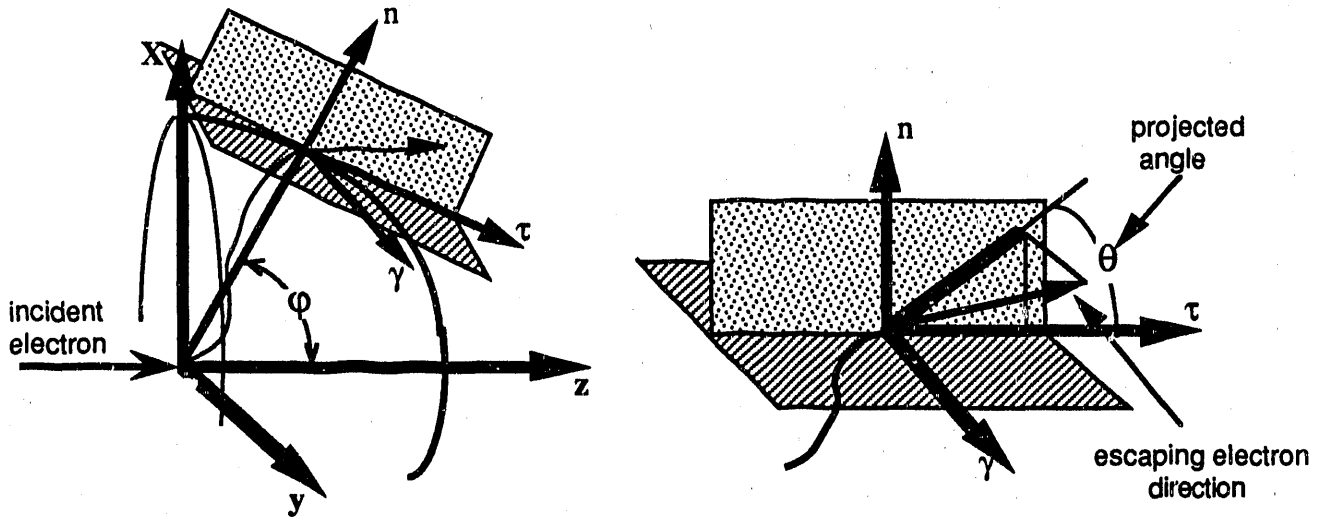


Figure 5. A Single Electron History in the Global Calculation.

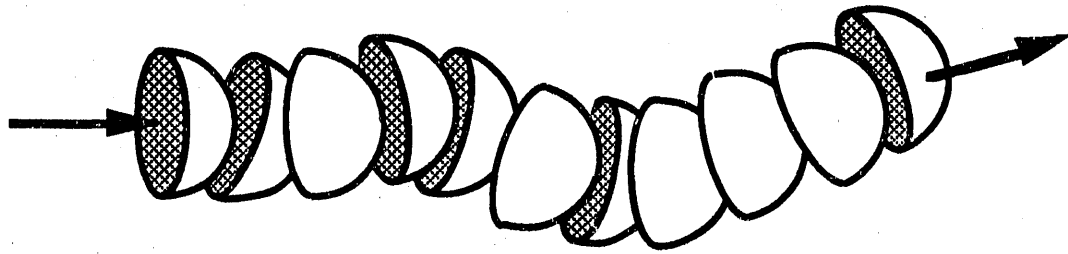


Figure 6. Backscatter Energy Spectrum for 10 keV Electrons Normally Incident on Thick Aluminum

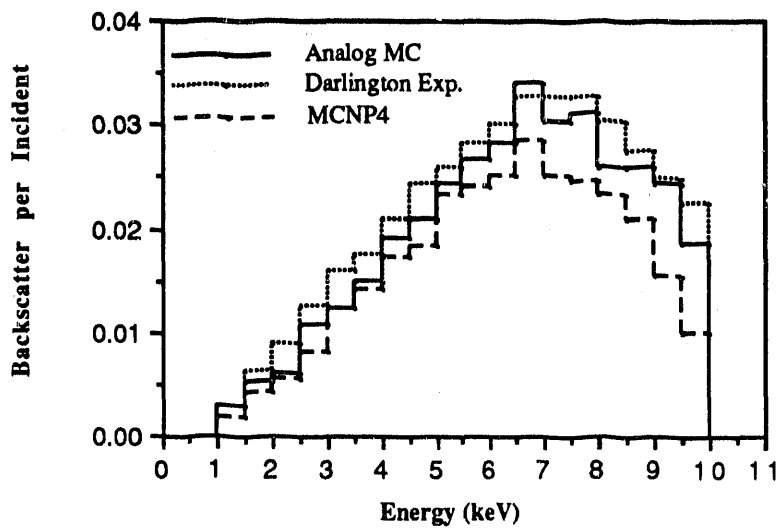


Figure 7. Backscatter Percentage Versus Incident Energy for Perpendicularly Incident Electrons.

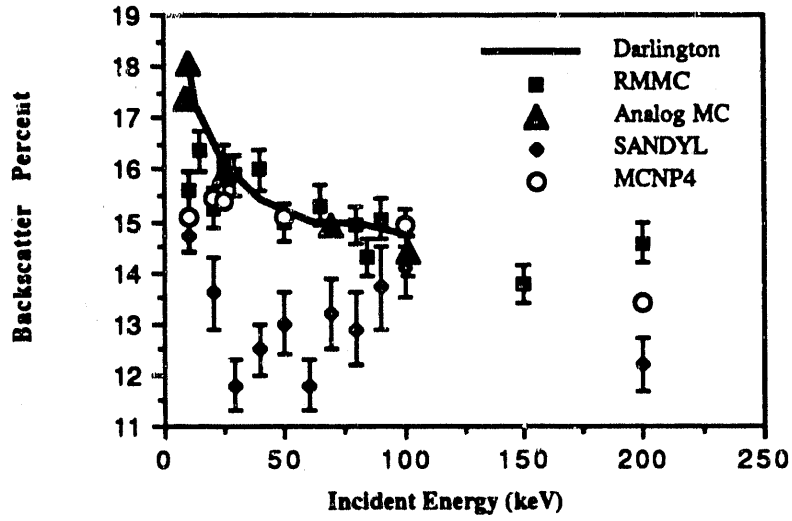
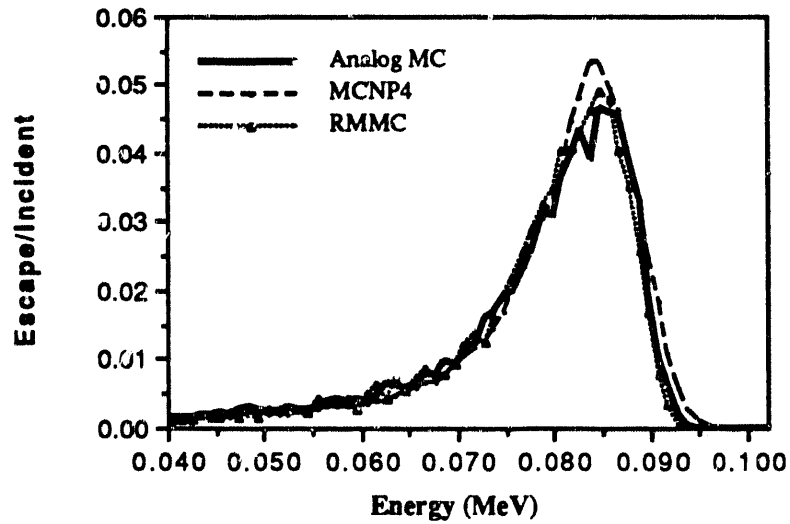


Figure 8. Energy Spectrum for Normally Incident 102 keV Electrons Transmitted Through 0.002 cm. of Aluminum



**END**

**DATE FILMED**

03 / 05 / 91

